Transactions of the Materials Research Society of Japan 29[5] 2251-2256 (2004)

Rational Design of Low-dimensional Nanomaterials: Novel Soft Solution Approaches*

Shu-Hong Yu *
Hefei National Laboratory for Physical Sciences at Microscale and Department of Materials Science and Engineering, University of Science and Technology of China
Fax: 86-551-3603040, e-mail: shyu@ustc.edu.cn

Nanosized building blocks with low dimensionality such as nanotubes, nanowires, nanorods, and ultra-thin nanosheets, have emerged as very technically important systems, which provide both fundamental scientific opportunities for investigating the influence of size and dimensionality on optical, magnetic and electronic properties and potential good components for significantly improving the material properties. The latest advances on new mild soft solution based strategies for fabrication of low dimensional nanocrystals such as hydrothermal/solvothermal processes will be addressed. The versatile rational synthetic strategies of a variety of low dimensional nanorods, nanowires, and nansheets, with controllable size, shape, and length scale using mild soft solution processes will be discussed. These low dimensional nanocrystals with special shape and structural features could find potential applications in nanoscience and nanotechnology.
Key words: low dimensional nanocrystals, soft solution processing, hydrothermal/solvothermal process.

1. INTRODUCTION

Low-dimensional materials such as nanometer-size inorganic dots, tubes, and wires exhibit a wide range of electronic and optical properties that depend sensitively on both size and shape, and are of both fundamental and technological interest [1, 2]. They are potentially ideal building blocks for nanoscale electronics and optoelectronics [3]. The ability to control the shapes of semiconductor nanocrystals affords an opportunity to further test theories of quantum confinement, and yields samples with desirable optical characteristics from the point of view of application [4,5].

Searching for new strategies toward one dimensional nanosized building blocks such as nanorods, nanowires, nanotubes, and nanobelts has attracted intensive interest because of their distinctive geometries, novel physical and chemical properties, and potential applications in nanodevices [3, 6]. These systems are expected to display the size and shape dependent optical, magnetic, and electronic properties [7, 8]. Exploration of new synthetic routes for preparing novel nanocrystals with structural specialty and complexity has been a recent focus [9,10,11].

A trend and challenging in synthetic chemistry and materials science is that how the traditional solid-state reaction can be conducted in round-bottom flasks (i.e. turning down the heat for fabrication of crystals) [12,13]. Recent development in soft solution processing may provide an alternative, convenient, lower temperature, and environmentally friendly pathway for fabrication of advanced ceramic materials with desirable shapes and sizes [14]. As one kind of solution-based chemical processes, hydrothermal process has been widely used for the synthesis of vast range of solid-state compounds.

Hydrothermal synthesis can be defined as the use of water as a solvent in a sealed reaction container when the temperature is raised above 100 °C. Under these conditions, autogeneous pressure (*i.e.* self-developing and not externally applied) is developed. The pressure within the sealed reaction container is found to increase dramatically with temperature, but also will depend on other experimental factors, such as the percentage fill of the vessel and any dissolved salts.

The use of hydrothermal conditions can exert significant effects on the reactivity of inorganic solids and the solubility of the compounds under conditions of elevated pressure and temperatures. The chemical reactivity of usually insoluble reagents can be much enhanced and a lot of sluggish solid state reactions can be initiated under hydrothermal conditions [15]. Usually, hydrothermal synthesis often applies higher temperatures (above 300 °C) and often took place in the supercritical regime. However, even milder reactions conditions (temperature < 250 °C) can be applied not only to provide a convenient low temperature route to materials with practical application, but also in the exploratory synthesis of new solids [16,17].

In recent years, the concepts embodied in hydrothermal process have been extrapolated to non-aqueous system, therefore, its counterpart so-called "*solvothermal process*" emerges, in which a organic solvent is used as reaction media instead of water at elevated temperature about its boiling point. As the counterpart of hydrothermal process, solvothermal process has emerged in recent years and has received great attention in synthetic chemistry and materials science.

In this paper, the recent development on hydrothermal process and its counterpart solvothermal process for the synthesis of advanced inorganic nanocrystals with special shape, phase, and dimensionality will be addressed. The progress on the shape control synthesis of various semiconductor nanocrystals will be summarized.

2. SHAPE AND PHASE CONTROL OF SEMICONDUCTOR NANOCRYATLS

2.1 II-VI group semiconductor nanocrystals

The shape, particle size, and phase of II-VI group semiconductor nanparticles can be controlled conveniently by solvothermal process [18, 19, 20]. CdS sample synthesized in ethylenediamine (en) via the reaction of CdC_2O_4 with sulfur at 160 °C for 12 h can be CdS crystallites synthesized in ethylenediamine are uniform nanorods with diameters of 20-50 nm and lengths of 200-1300 nm as shown in Fig. 1a. In addition, the CdS crystallites synthesized in other polyamines such as diethylene triamine (dien) and triethylene tetraamine (trien) under the same experimental conditions display the same morphology. However, the CdS powders obtained in dien consist of uniform nanorods with diameters 30-60 nm and lengths of 200-4800 nm. Wurtzite CdSe nanorods with diameter 6-20 nm and lengths up to 100-500 nm can also be synthesized in en, dien, and trien.

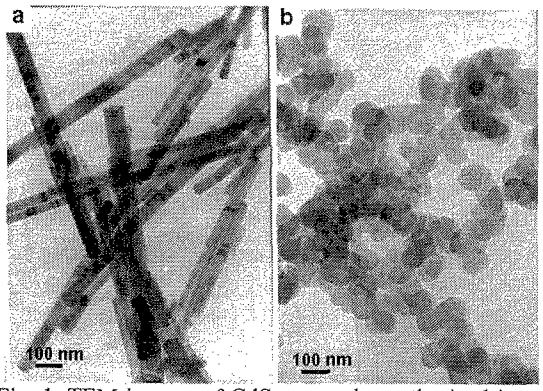

Fig. 1. TEM images of CdS nanorods synthesized in en at 160 °C for 12 h. (b) Disk-like CdS nanoparticles synthesized in pyridine at 160 °C for 12 h.

The solvothermal reaction of zinc salts such as $Zn(CH_3COO)_2 \cdot 2H_2O$ or $ZnCl_2$, and with thiourea in ethylenediamine (en) at 120-180 °C for 6-12 h results in sheet-like nanosheets with a composition ZnS • $(en)_{0.5}$ [21]. Pure wurtzite ZnS (W) nanosheets with rectangle lateral dimensions in a range of 0.3-2 μm.can be produced from removing the ethylenediamine (en) by thermal decompostion at 250-500 °C under vacuum as shown in Fig. 2a The oxidization of the lamellar molecular in air produced wurtzite ZnO flake-like dendrites. The nanosheets are well crystallized single crystals with growth direction along *a* and *c* axis as indicated by the SAED pattern in Fig. 2a. HRTEM image show well resolved (100) lattice planes with lattice spacing 3.3 Å, indicating that the preferred orientation along *a* axis (Fig. 2b).

The shape evolution process of CdS nanorods in ethylenediamine media has been carefully investigated [20]. There are two possible coordination modes between Cd^{2+} on the surface and ethylenediamine (en) molecules, i.e., monodentate (Scheme 2a) or bridging (Scheme 2b). The results suggest that the *trans*-conformation of en molecule adsorbed on the surface of CdS plays an important role in the formation of CdS nanorods.

The sythetic method is both flexible and reproducible for controlling the phase, shape, and sizes of ZnS nanocrystals. By the similar solvothermal reation at 120 °C using ethanol instead of ethylenediamine as solvent, sphalerite ZnS (S) nanoparticles with size of ~ 3 nm can be easily synthesized. In addition, wurtzite ZnS nanorods can also be synthesized by using *n*-butylamine, a monodentate amine, as solvent (Fig. 3). In addition, the nanorods could be aligned together to form bundle structures or arrays under limited experimental conditions. The detailed study shows that the phase and shape of ZnS nanocrystals can be well controlled by choosing suitable solvent. A rational design of solvothermal reaction allows it possible to control both the dimensionality (dots, rods, and sheets) of ZnS nanocrystals and the phase as illustrated in Scheme 1.

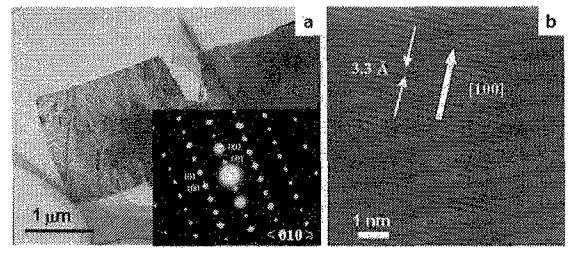

Fig. 2. TEM images and SAED patterns for (a) wurtize ZnS single crystal nanosheets obtained by thermal decomposition of lamellar ZnS • $(en)_{0.5}$ precursor at 500 °C for 0.5 h in vacuum; inserted SEAD pattern recorded along <010> zone. (b) HRTEM image of the wurtize ZnS single crystal nanosheet.

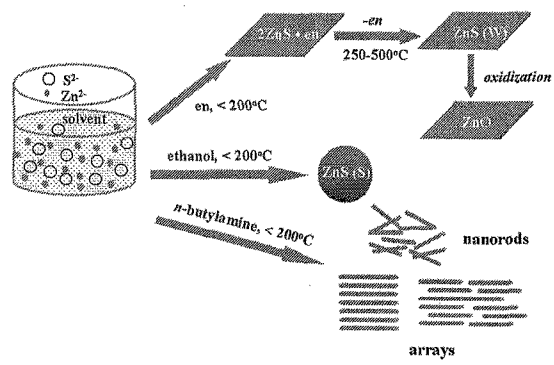

Scheme 1. The illustration of controlled synthesis of ZnS nanocrystals with different dimensionalities and phases: ZnS dots, nanosheets, nanorods, and bundles.

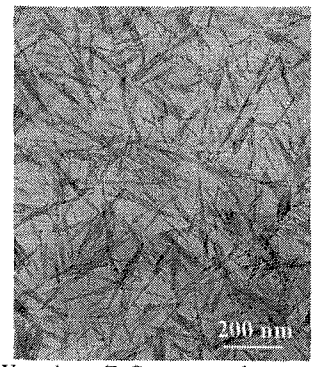

Fig. 3. Wurtzite ZnS nanorods synthesized in *n*-butylamine at 250 °C for 12 h.

It has been shown that monodentate amine such as *n*-Butylamine can also be used as reaction media for the synthesis of various semiconductor nanorods. *n*-Butylamine acts as a monodentate ligand, the coordination between it and metal ions must be in a monodentate mode, as shown in Scheme 2c. In order to verify whether monodentate ligand can be used as "*shape controller*" for synthesis of other semiconductor nanorods, a series of similar solvothermal reactions were performed in *n*-butylamine [22]. A mixture of hexagonal phase CdSe and cubic phase CdSe was obtained at 160 °C for 12 h. The CdSe nanocrystals are composed of nanorods with 12~16 nm in width and 200~400 nm in length. Simliarly, wurtzite ZnSe nanoparticles can also be obtained at 220 °C for 12 h. The ZnSe nanocrystals are composed of nanorods with diameters in the range of 25~50 nm and lengths up to 1000 nm. A well-crystallized single ZnSe nanorod with the growth direction along *c* axis is presented in Fig. 4b. The wurtzite ZnSe nanorods was achieved for the first time in solution system under mild considition. Cubic PbSe nanorods with 12~20 nm in width and 200~450 nm in length as shown in Fig. 4c can be obtained at 80 °C for 12 h. The growth direction of the nanorods was along <200>. These results indicate that selecting the proper experimental conditions is important for the formation of nanorods, although nanorods can be synthesized in *n*-butylamine.

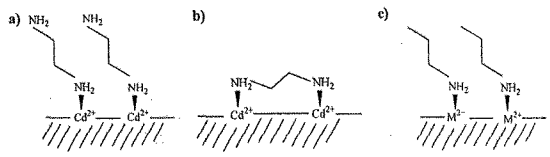

Scheme 2. Illustration on the possible coordination mode on the surface (a) monodentate mode of en molecules. (b) polydentate mode of en molecules. (c) monodentate mode of *n*-butylamine.

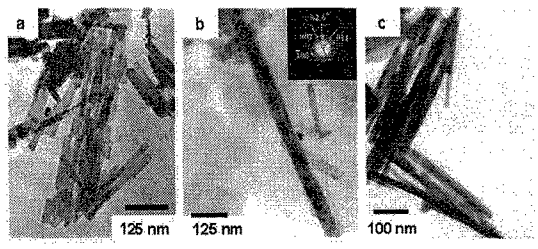

Fig. 4. TEM images of (a) CdSe nanocrystals (160 °C, 12 h); (b) ZnSe nanocrystals, (220 °C, 12 h); (c) PbSe nanocrystals (80 °C, 12 h).

This solvent-mediated controlling mechanism has been demonstrated to be successful in synthesis of a variety of semiconductor nanorods/nanowires. In this mechanism, ligands control the shape of nanocrystals through the interaction between ligands and metal ions on the surface of nuclei. One anchor atom in a ligand such as *n*-butylamine is necessary but suifficent for the formation of 1D nanocrystals, even though more anchor atoms may be present in a ligand. The close interaction between anchor atoms in ligands and metal ions on the surface is another important prerequisite for nanorod formation. Furthermore, this route provides not only a possible general route to other chalcogenide nanorods in large scale but also a guide for further rational design of 1D chalcogenides.

2.2 V-VI group semiconductor nanorods

1D $A^{V}_{2}B^{VI}_{3}$ (A = Sb, Bi, As and B = S, Se, Te) semiconductor nanorods can also be synthesized by solvothermal process [23-, 24, 25]. In order to avoid the hydrolysis of the bismuth and antimony salts in the presence of water, a so-called solvothermal decomposition process (SPD) was developed for fabrication of Bi_2S_3 and Sb_2S_3 nanowires (or nanorods) [24], using $BiCl_3$ or $SbCl_3$ and thiourea (Tu) or thioacetamide (TAA) as starting reactants in polar solvents:

$$M^{3+} + Tu \xrightarrow{solvent} M_2S_3\,(1D) \quad (M = Bi, Sb)$$

The controllable synthesis of Bi_2S_3 nanocrystals with different size and aspect ratios were illustrated in Scheme 3 and Fig. 5. Bi_2S_3 nanowires/nanorods with controllable sizes can be selectively synthesized conveniently by solvothermal decomposition process (SDP) and hydrothermal process under suitable conditions [23-,24,25].

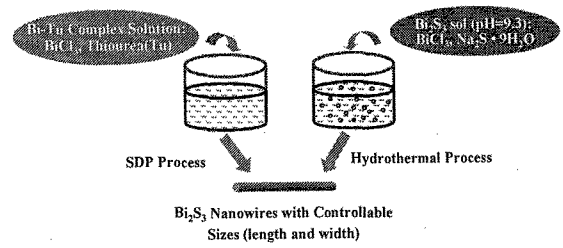

Scheme 3. Schematic illustration for preparation of Bi_2S_3 nanowires with controllable sizes.

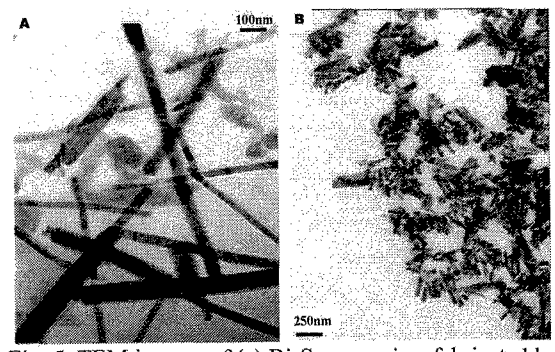

Fig. 5. TEM images of (a) Bi_2S_3 nanowires fabricated by solvothermal decomposition process at 140 °C, 12 h, ethanol. (b) rod-like Bi_2S_3 particles prepared by hydrothermal treatment of the sol (pH = 9.3) at 150 °C for 6 h.

Sb_2S_3 nanorods can also be easily produced with high yield by use of the same procedure [26]. The time-dependent of the shape evolution of the nanocrystals during the crystallization has been studied, indicating that the transformation from amorphous nanoparticles to crystallized nanorods is much faster in a closed system than that in an open system [26].

2. FINE TURNING OF NANOSTRUCTURES BY BLOCK COPOLYMERS

Very thin 1D and 2D $CdWO_4$ nanocrystals with controlled aspect ratios were conveniently synthesized at ambient temperature or by hydrothermal ripening under control of double hydrophilic block copolymer [27].

TEM image in Fig. 6a shows very thin, uniform $CdWO_4$ nanorods/nanobelts with lengths in the range of 1 to 2 μm and a uniform width of 70 nm along their entire length (aspect ratio of about 30). The thickness of the nanobelts is *ca* 6-7 nm. The slow and controlled reactant addition by the doube-jet technique under stirring mainains formation of intermediate amorphous nanoparticles at the jets [28] so that nanoparticles are the precursors for the further particle growth rather than ionic species. Successive hydrothermal ripening after the double jet reaction leads to a rearrangement of the rods into 2D lens-shaped, raft-like superstructures with a resulting lower aspect ratio. In contrast, very thin and uniform nanofibers with a diameter of 2.5 nm, a length of 100-210 nm, and an aspect ratio of 40-85 as shown in Fig. 6b can be readily obtained when the double hydrophilic block copolymer poly(ethylene glycol)-*block*-poly(methacrylic acid (PEG-*b*-PMAA) was added to the solvent reservoir before the double-jet crystallization process and the mixture was then hydrothermally ripened at 80 °C.

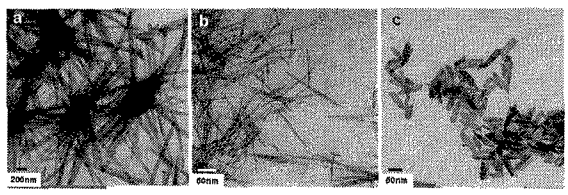

Fig. 6. TEM images of the $CdWO_4$ nanocrystals obtained under different conditions. (a) No additives, double jet, at room temperature. (b) in the presence of PEG-*b*-PMAA (1 g L^{-1}), 20 mL, double jet, then hydrothermal crystallization at 80 °C for 6 h. (c) direct hydrothermal treatment of 20 mL solution at 130 °C for 6 h, in the presence of 1 g L^{-1} PEG-*b*-PMAA-PO_3H_2. pH = 5.3, $[Cd^{2+}]:[WO_4^{2-}] = 8.3 \times 10^{-3}$ M (final solution).

When the partly phosphonated hydrophilic block copolymer PEG-b-PMAA-PO_3H_2 (21%) (1 g L^{-1}) is added at an elevated temperature of 130 °C even without using the double jets but at higher concentrations and coupled supersaturation, very thin platelet-like particles with a width of 17-28 nm, a length of 55-110 nm, and an aspect ratio of 2-4 are obtained by a direct hydrothermal process as shown in Fig. 6c. The results indicated that $CdWO_4$ nanostructures can be fine-turned by use of block copolymers.

3. GENERAL SYNTHESIS OF TUNGSTATE AND MOLYDBATE NANORODS/NANOWIRES

General synthesis of a family of single crystalline transition metal tungstate nanorods/nanowires in large scale has been realized recently by a facile hydrothermal crystallization technique under mild conditions using cheap and simple inorganic salts as precursors [29]. Uniform tungstate single crystal nanorods/nanowires such as MWO_4 (M = Zn, Mn, Fe), Bi_2WO_6, Ag_2WO_4, and $Ag_2W_2O_7$ with diameter 20-40 nm and length up to micrometers and controlled aspect ratios can be readily obtained by hydrothermal transformation and re-crystallization of amorphous particulates.

The pH value of precursor medium plays a crucial effect on both the formation of tungstate phase and their morphology in this system. In addition, the aspect ratio of $ZnWO_4$, $FeWO_4$, and $MnWO_4$ nanorods/nanowires strongly depends on the initial pH value of the dispersion.

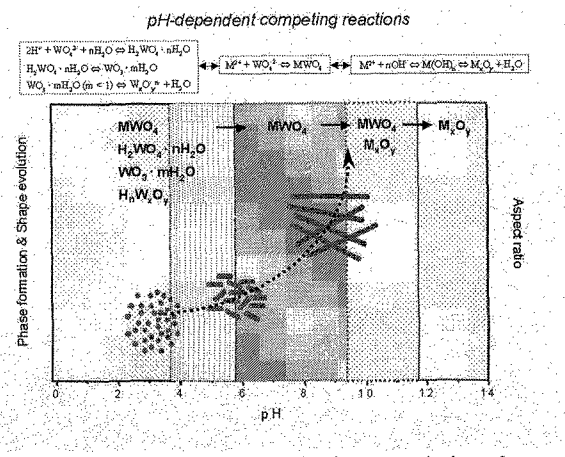

Fig. 7. The map of shape and phase evolution for tungstate materials by hydrothermal crystallization process.

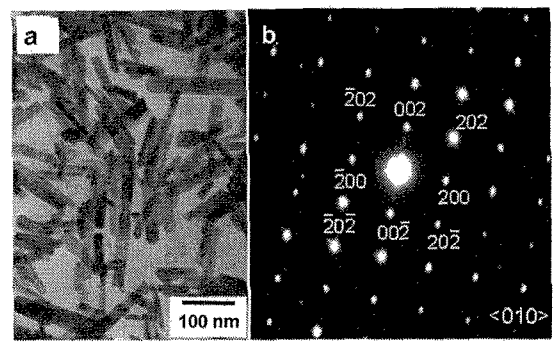

Fig. 8. (a) TEM image of $MnWO_4$ nanorods, pH 9, 180 °C, 12 hours. $[Mn^{2+}]$: $[WO_4^{2-}]$ = 1:1. (b) ED pattern taken along <010> zone.

The phase formation zone and the shape evolution can be mapped as shown in Fig. 7 based on large amount of experimental data obtained for various tungstate compounds by variation of pH and the compositions of the starting dispersions. In addition, the temperature also has significant influence on the formation of the nanorods. The fundamental results show that the products obtained at lower temperature as low as 120 °C under the identical solution conditions can only produce near spherical aggregates, which are composed of tiny nanoparticles. The optimum temperature for rapid production of high crystalline nanorods is as high as 180 °C. Single crystals of $MnWO_4$ nanorods with diameter 25 nm and length 100-150 nm were obtained at pH 9 (Fig. 8a). Electron diffraction pattern in Fig. 8b reveals the perfect single-crystalline nature of the nanorods with the preferential growth along [100] direction.

Recent work shows that this approach can be extended further for the general synthesis of various

molydbates nanorods/nanowires, as well as rare earth compounds with interesting shape, phase, and nanostructures.

Selective synthesis of uniform single crystalline silver molybdate/tungstate nanorods/nanowires in large scale can be realized by a facile hydrothermal re-crystallization technique [30]. Similar to the tungstate system, the synthesis is found to be strongly dependent on pH, temperature, and reaction time. Extremely long $Ag_6Mo_{10}O_{33}$ single crystal nanowires covered with a lot of tiny nanoparticles can be obtained at pH 2 as shown in Fig. 9. Electron diffraction pattern taken along [100] zone axis indicated that the nanowires are perfect single crystals.

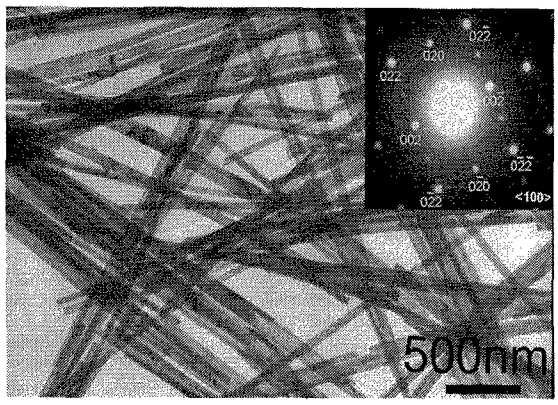

Fig. 9. TEM image and electron diffraction pattern of $Ag_6Mo_{10}O_{33}$ nanowires. $[AgNO_3]$ = 0.1 M, $[(NH_4)_6Mo_7O_{24}]$ = 0.014 M, pH 2, 140 °C, 12 h. Electron diffraction pattern was taken along [100] zone axis.

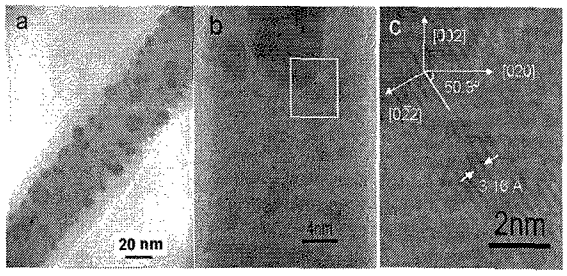

Fig. 10. High magnification TEM images of the $Ag_6Mo_{10}O_{33}$ nanowires obtained at pH 2, $[AgNO_3]$ = 0.1 M, $[(NH_4)_6Mo_7O_{24}]$ = 0.014 M, 140 °C, 12 h: (a)-(b) high resolution image show the surface structures of the nanowires after exposed electron beams. (c) Lattice resolved HRTEM image, showing that the nanowires grow along [002].

High resolution TEM image shows that very tiny nanoparticles with size of 5 nm attached on the backbone of the $Ag_6Mo_{10}O_{33}$ nanowires. Interestingly, after exposed under TEM electron beams, a lot of tiny nanoparticles appeared on the backbone of the nanowires (Fig. 10a). It is believed that the $Ag_6Mo_{10}O_{33}$ nanowires are not stable under electron beam irradiation. After exposed for longer time, many tiny nanoparticles appeared on the wire surfaces and these particles tend to become amorphous as confirmed by electron diffraction observation. The lattice resolved HRTEM image was shown in Fig. 10b-c. The lattice spacing 3.16 Å corresponding to that for $(0\bar{2}2)$ planes. The calculated angle between (002) and $(0\bar{2}2)$ is 50.3°, which is consistent with that observed in Fig. 10c. In addition, the angle between (020) and $(0\bar{2}2)$ is 148.4 °, which fits the measured value very well too. These results suggested that the nanowires grow preferentially along *c* axis. TG-DTA analysis shows that the melting point of this compound is about 238 °C, suggesting that the nanowires could be destroyed under too longer electron beam irradiation.

The access toward various kinds of low dimensional tungstate nanocrystals under mild conditions could open new opportunities for further investigating the novel properties of tungstate materials due to their decreasing dimensionalities. The results demonstrated that it is possible to selectively synthesize other family of molybdate nanowires with controllable phases and structural specialty. The discovery of this new family of molybdate nanowires could lead to new applications of these materials. Furthermore, these new families of 1D nanoscale building blocks could further act as 1D nanoscale building blocks for synthesis of other more complex oxide nanostructures, which would bring us a rich nanochemistry about tungstates, molybdates, and their derivates, and thus could result in new opportunities for potential applications.

4. SUMMARY AND OUTLOOK

Solvothermal/hydrothermal processes have shown the potential possibilities and versatilities for selective synthesis of various nanocrystals. The feasibility and capability of solvothermal/hydrothermal approaches are worth being explored for other inorganic systems since it symbolizes an efficient mild solution way toward rational designing low dimensional nanocrystals in large scale with promising advantages in contrast to previous high temperature approaches.

The successful synthesis of various semiconductor nanorods/nanowires by using suitable ligand solvent as "*shape-controller*" indicates that solvothermal process symptomatized a fruitful and promising route toward 1D and 2D semiconductor nanocrystals. Current progress has demonstrated that solvothermal process has become a fruitful route for synthesis of various non-oxides materials with special shape, controllable sizes and phases, which may add new variables in tailoring the materials properties and stimulate further research into the correlation of the shape, sizes, and phases of the nanomaterials with their properties.

Although these processes have shown promising future in synthesis of materials, they are not yet well established, i.e., the chemical reactivity, reaction mechanism, and the role of solvents in the reactions are very complicated and still not clear, which no doubt need to be resolved in future. Further understanding on the nucleation, crystallization, self-assembly, and growth mechanism of the nanocrystals in solution strategies should improve the current synthesis and could open new rational pathways to prepare various kinds of low dimensional nanocrystals with high quality.

* S.-H. Yu acknowledges the special funding support from the Century Program of the Chinese Academy of Sciences and the Natural Science Foundation of China (the Distinguished Yong Fund of the National Science Foundation of China (NSFC), and Project No. 50372065) for financial support..

REFERENCES

[1] J. T. Hu, T. W. Odom and C. M. Lieber, *Acc. Chem. Res.*, 32, 435-445 (1999).
[2] C. M. Lieber, *Solid State Commun.*, 107, 607-616 (1998).
[3] X. Duan, Y. Huang, Y. Cui, J. Wang and C. M. Lieber, *Nature*, 409, 66-69 (2001).
[4] K. Leung, S. Pokrant and K. B. Whaley, *Physical. Rev. B* 57, 12291-2301 (1998).
[5] X. G. Peng, L. Manna, W. D. Yang, J. Wickham, E. Scher, A. Kadavanich and A. P. Alivisatos, *Nature*, 404, 59-61 (2000).
[6] A. P. Alivisatos, *Science*, 271, 933-37 (1996).
[7] T. S. Ahmadi, Z. L. Wang, T. C. Green, A. Henglein and M. A. EI-Sayed, *Science*, 272, 1924-26 (1996).
[8] Y. Cui, Q. Q. Wei, H. K. Park, C. M. Lieber, *Science*, 293, 1289-292 (2001).
[9] P. D. Yang, Y. Y. Wu, R. Fan, *International Journal of Nanotechnology*, 1, 1-41 (2002).
[10] Y. N. Xia, P. D. Yang, Y. G. Sun, Y. Y. Wu, B. Mayers, B. Gates, Y. D. Yin, F. Kim and H. Q. Yan, *Adv. Mater.*, 15, 353-389 (2003).
[11] G. R. Patzke, F. Krumeich and R. Nesper, *Angew. Chem. Int. Ed.*, 41, 2447-461 (2002).
[12] A. Stein, S. W. Keller and T. E. Mallouk, *Science*, 259, 1558-564 (1993).
[13] W. E. Buhro, K. M. Hickman and T. J. Trentler, *Adv. Mater.* **8**, 685-690 (1996).
[14] M. Yoshimura, W. Suchanek and K. Byrappa, *MRS Bull.*, 9, 17-21 (2000).
[15] S. H. Yu, *J. Ceram. Soc. Jpn.*, 109, S65-75 (2001).
[16] S. Feng and R. Xu, *Acc. Chem. Res.* 34, 239-247 (2001).
[17] R. I. Walton, *Chem. Soc. Rev.*, 31, 230-38 (2002).
[18] S. H. Yu, Y. S. Wu, J. Yang, Z. H. Han, Y. Xie, Y. T. Qian and X. M. Liu, *Chem. Mater.*, 10, 2309-312 (1998).
[19] S. H. Yu, J. Yang, Z. H. Han, Yong Zhou, Ru-Yi Yang, Yi Xie, Yi-Tai Qian and Yu-Heng Zhang, *J. Mater. Chem.*, 9, 1283-89 (1999).
[20] J. Yang, J. H. Zeng, S. H. Yu, L. Yang, G. E. Zhou and Y. T. Qian, *Chem. Mater.*, 12, 3259-263 (2000).
[21] S. H. Yu and M. Yoshimura, *Adv. Mater.*, 14, 296-300 (2002).
[22] J. Yang, C. Xue, S. H. Yu, J. H. Zeng and Y. T. Qian, *Angew. Chem. Ed. Int.*, 41, 4697-700 (2002).
[23] S. H. Yu, Y. T. Qian, L. Shu, Y. Xie, L. Yang and C. S. Wang, *Mater. Lett.*, 35, 116-19 (1998).
[24] S. H. Yu, L. Shu, J. Yang, Z. H. Han, Y. T. Qian and Y. H. Zhang, *J. Mater. Res.*, 14, 4157-162 (1999).
[25] S. H. Yu, J. Yang, Y. S. Wu, Z. H. Han, Y. Xie and Y. T. Qian, *Mater. Res. Bull.*, 33, 1661-666 (1998).
[26] J. Yang, J. H. Zeng, S. H. Yu, L. Yang, Y. H. Zhang and Y. T. Qian, *Chem. Mater.*, 12, 2924- 29 (2000).
[27] S. H. Yu, M. Antonietti, H. Cölfen and M. Giersig, *Angew. Chem. Int. Ed.*, 41, 2356-60 (2002).
[28] H. Cölfen and M. Antonietti, *Langmuir*, 14, 582-89 (1998).
[29] S. H. Yu, B. Liu, M. S. Mo, J. H. Huang, X. M. Liu and Y. T. Qian, *Adv. Funct. Mater.*, 13, 639-647 (2003).
[30] X. J. Cui, S. H. Yu, L. L. Li, L. Biao, H. B. Li, M. S. Mo and X. M. Liu, *Chem. Eur. J.*, 9, 218-223 (2003).

(Received October 11, 2003; Accepted March 17, 2004)